Applied Surface Science 602 (2022) 154150

Contents lists available at ScienceDirect

Applied Surface Science

journal homepage: www.elsevier.com/locate/apsusc

Full length article

From molecular adsorption to decomposition of methanol on various ZnO facets: A periodic DFT study

Shweta Mehta, Kavita Joshi *

Physical and Materials Chemistry Division, CSIR-National Chemical Laboratory, Dr. Homi Bhabha Road, Pashan, Pune 411008, India
Academy of Scientific and Innovative Research (AcSIR), Sector 19, Kamla Nehru Nagar, Ghaziabad, Uttar Pradesh 201002, India

ARTICLE INFO

Keywords:
DFT
Surface interactions
ZnO
MeOH

ABSTRACT

Methanol is an interesting and important molecule to study because of its potential to replace existing fuels. It is also a prominent hydrogen source which can be used to generate hydrogen in-situ. ZnO is widely used as catalyst in synthesis of methanol from CO_2 at industrial scale. In this work, we demonstrate that the same catalyst could be used for MeOH decomposition. We have investigated interaction of methanol with various flat and stepped facets of ZnO by employing Density Functional Theory (DFT). Two flat [$(10\bar{1}0)$ and $(11\bar{2}0)$] and two stepped [$(10\bar{1}3)$ and $(11\bar{2}2)$] facets are studied in detail for methanol adsorption. Chemisorption of MeOH with varying strength is common to all four facets. Most importantly spontaneous dissociation of O-H bond of methanol is observed on all facets except $(11\bar{2}0)$. Our DFT calculations reveal that molecular adsorption is favored on flat facets, while dissociation is favored on step facets. Also, $(10\bar{1}0)$ facet undergoes substantial reconstruction upon MeOH adsorption. Activation of C-H bond along with strengthening of C-O bond on ZnO facets suggest partial oxidation of methanol. With our DFT investigations, we dig deeper into the underlying electronic structure of various facets of ZnO and provide rationale for the observed facet dependent interaction of ZnO with MeOH.

1. Introduction

Methanol is one of the most important chemical for industrial reactions and a primary feed-stock for energy production. Due to easier transportation and compatibility with the existing infrastructure, methanol attracts considerable attention. Methanol emerges as an efficient means to store energy and it can also be used as a convenient fuel [1]. It is also used in the direct methanol fuel cell (DMFC). Methanol can also be converted to various hydrocarbons like formaldehyde, dimethyl ether, etc. Methanol is also a promising hydrogen source because of its high hydrogen content [2,3]. However, use of methanol as a source of hydrogen requires breaking of its O-H and C-H bonds with substantial bond dissociation energies, viz. 96.1 kcal/mol and 104.6 kcal/mol respectively [4]. Over the past two decades, extensive studies of activation and decomposition of methanol on various metal surfaces [5–15], metal alloys [16–21], metal clusters [22–25], metal oxides [26–32], mixed metal oxides [33], and zeolites [34–36] have been carried out. In general metal oxides turn out to be better catalyst for activation of methanol due to the presence of oxygen on the surface, which acts as an active site.

As discussed above, breaking bond of methanol is primary step to convert it to any value added product. The industrial catalyst used for synthesis of methanol from syn gas is Cu-ZnO/Al_2O_3. In a recent computational study, Elnabawy et al. demonstrated the role of ZnO in industrial catalyst for methanol synthesis [37]. They reported that the strong metal support interaction between Cu and ZnO favors higher activity towards methanol synthesis. ZnO reduces and partially covers the Cu surface which causes modification in the surface. However, the active Cu sites remain unaffected leading to higher activity of catalyst. ZnO is considered as a very active catalyst for many reactions because of its mixed covalent and ionic bonding [38]. Industrially methanol is partially oxidized to formaldehyde using two different catalyst, silver or iron-molybdenum oxides. However, the reaction takes place at elevated temperatures in both the cases. It is as high as 600°C when silver is used as catalyst whereas it drops down to ~ 250–400°C for molybdenum catalyst. Clearly there is a room for improvement of the catalyst which could bring down the reaction temperature further. In an experimental study, Boisen et al. demonstrated that optimal ammonia synthesis catalyst is not the optimal ammonia decomposition catalyst [39]. Contrary to that, ZnO, which is an optimal methanol synthesis catalyst exhibits excellent activity for methanol decomposition. Vo et al. investigated the adsorption

* Corresponding author at: Physical and Materials Chemistry Division, CSIR-National Chemical Laboratory, Dr. Homi Bhabha Road, Pashan, Pune 411008, India.
E-mail addresses: sk.mehta@ncl.res.in (S. Mehta), k.joshi@ncl.res.in (K. Joshi).

https://doi.org/10.1016/j.apsusc.2022.154150
Received 1 March 2022; Received in revised form 3 June 2022; Accepted 1 July 2022
Available online 13 July 2022

and decomposition of methanol on ZnO($10\bar{1}0$) by employing DFT and concluded that methanol strongly adsorbed on ZnO($10\bar{1}0$) surface as compared to CuCl(111), Cu(111), and Au(111) surfaces. Their results showed that decomposition of MeOH to CH_2O molecule has a barrier of 1.20 eV [40]. In another interesting study, Abedi et al. employed DFT to understand the conditions leading to monolayer formation of methanol on ZnO($10\bar{1}0$) surface. They reported breaking of the O-H bond, with a barrier of 0.5 eV, as the preferred mechanism over cleavage of C-O bond [41]. In a combined experimental and theoretical work, Ruan et al. used high-resolution scanning tunneling microscopy in combination with density functional theory to identify both the physi- and chemisorbed methanol species on the non-polar ZnO($10\bar{1}0$) surface. The physisorption of methanol dominates at liquid nitrogen temperature which transform into chemisorption upon either thermal annealing or electron injection. Moreover, the chemisorbed methanol mostly retains an undissociated state and tends to form one-dimensional chain structure along the (0001) direction mediated by the intermolecular hydrogen bonding interactions [42]. A DFT study carried out by Smith et al. demonstrated significantly lower reaction barrier (0.39 eV) towards methanol dissociation on ZnO (0001) compared to PdZn surfaces (0.54 eV) [43]. Recently Jin et al. studied the adsorption and reactions of CH_3OH on non-polar mixed-terminated ZnO($10\bar{1}0$), polar O terminated ZnO($000\bar{1}$) and Zn terminated ZnO(0001) surfaces using high-resolution electron energy loss spectroscopy (HREELS) in conjunction with temperature programmed desorption (TPD). They found that for all three ZnO surfaces, methanol adsorb dissociatively at room temperature which leads to the formation of hydroxyl and methoxy species. Upon heating to higher temperatures (370 K and 440 K), the dissociated and intact methanol species on ZnO($10\bar{1}0$) predominantly undergo molecular desorption releasing CH_3OH. While on both polar surfaces, thermal decomposition of CH_3OH occurs to produce CH_2O, H_2, CO, CO_2, and H_2O at temperatures higher than 500 K [44].

Although ZnO is used extensively as a catalyst in many reactions, its potential is not truly realized. To the best of our knowledge only non-polar ($10\bar{1}0$) and polar (0001) facets of ZnO have been studied for methanol activation. XRD pattern shows that ($11\bar{2}0$), ($10\bar{1}3$), and ($11\bar{2}2$) are also prominent facets. These facets are hardly studied for methanol activation. In the present work, we have systematically studied the interaction of methanol with various flat ($10\bar{1}0$), ($11\bar{2}0$) and stepped surfaces ($10\bar{1}3$), ($11\bar{2}2$) by employing periodic DFT. We report not only molecular adsorption and activation of O-H bond of methanol on these facets but also spontaneous dissociation of its O-H bond leading to formation of methoxy species. The quenched C-O bond-length in methanol along with partial double bond type character indicates onset of oxidation of methanol. We also demonstrate various possibilities regarding interaction of MeOH with ZnO and bring out the rationale behind the reactivity in terms of electronic structure of these facets. Finally we would like to bring out the role of computation in designing catalyst. DFT based computation has played a crucial role in rational design of catalyst while understanding its catalytic activity. To understand why different facets interact differently with MeOH, it is indispensable to investigate the underlying electronic structure. As we will demonstrate in the next section, our work brings out the possibility of ZnO being a suitable catalyst for MeOH decomposition as well. We also demonstrate that with distinguishable trends in the *p*DOS, charge transfer and other computed properties, we could explain variation in the interaction of methanol with different facets.

2. Computational details

All the calculations are carried out within the Kohn–Sham formalism of Density Functional Theory. Projector Augmented Wave potential [45,46] is used, with Perdew Burke Ernzerhof (PBE) [47] approximation for the exchange–correlation and generalized gradient approximation [48], as implemented in planewave, pseudopotential based code, Vienna Ab initio Simulation Package (*VASP*) [49–51]. The bulk unit cell is taken from the materials project [52]. The bulk lattice parameters upon optimization are a = 3.28 Å and c = 5.30 Å demonstrate excellent agreement with the experimentally measured (a = 3.24 Å, c = 5.20 Å) lattice parameters [53,54]. Two flat facets, ($10\bar{1}0$) and ($11\bar{2}0$) of ZnO are modeled as slabs by cleaving a surface with 3×3 periodicity in x and y direction with 4 layers using Quantumwise-VNL-2017.1 [55]. Two stepped facets, ($10\bar{1}3$) and ($11\bar{2}2$) are also cleaved by taking 3×1 and 2×2 periodicity respectively in the x and y direction with 6 layers. In every model, bottom layer is fixed and rest all layers and adsorbate are fully relaxed. Van der Waals corrections are applied to account for dynamic correlations between fluctuating charge distribution by employing Grimme method (DFT-D2) [56]. It is observed that 20 Å of vacuum is sufficient to avoid interaction between adjacent images of planes along the z-direction. Geometry optimization is carried out with a force cutoff of 0.01 eV/Å on the unfixed atoms and the total energies are converged below 10^{-4} eV for each SCF cycle. A Monkhorst–Pack grid of $3 \times 2 \times 1$ for ($10\bar{1}0$) and $3 \times 3 \times 1$ for ($11\bar{2}0$) slabs is used. For both stepped surfaces, Monkhorst–Pack grid of $2 \times 2 \times 1$ is used. The difference in energies is less than 4meV/atom for every system upon refining the K mesh further. Entire surface is scanned by placing MeOH molecule at all available unique sites. To compare the interaction of methanol at these sites, interaction energy is calculated using the formula: $E_{int} = E_{system} - (E_{surface} + E_{molecule})$ where E_{system} is energy of the system when MeOH is placed on the surface, $E_{surface}$ is energy of the bare surface and $E_{molecule}$ is energy of the MeOH molecule. To understand the electronic structure of these facets, total Density of States (*tDOS*) are calculated with denser k-mesh using LOBSTER [57–60]. Mulliken charges are computed for all the atoms on the surface.

3. Results and discussion

Bulk ZnO crystallizes in the hexagonal wurtzite structure consisting of hexagonal Zn and O planes stacked alternately. Both oxygen and zinc atoms are coordinated by four zinc and oxygen atoms respectively. Polar ((0001) and ($000\bar{1}$)) and non-polar (($10\bar{1}0$), ($10\bar{1}1$), ($11\bar{2}0$), ($10\bar{1}3$), and ($11\bar{2}2$)) facets have prominent peaks in XRD [61,62]. In this work, we have studied the interaction of methanol with two flat (($10\bar{1}0$), ($11\bar{2}0$)) and two stepped (($10\bar{1}3$), ($11\bar{2}2$)) facets of ZnO. The top and side view of all these facets are shown in Fig. SI1 and Fig. SI2. Each layer of ($10\bar{1}0$) is divided into two sub-layers leading to various unique sites for methanol adsorption. All these unique sites such as top of Zn, bridge of Zn-Zn, O-O, Zn-O, and bridge positions of atoms of two sub-layers are scanned for methanol interaction. All the sites where MeOH is placed are shown schematically in Fig. SI3. The numbers in Fig. SI3-(a) represent the initial positions where MeOH is placed and final position of adsorbed methanol or dissociated methoxy group are shown in Fig. SI3-(b). The black numbers indicate molecular adsorption while the red numbers denote dissociated methoxy group.

Before discussing the results in detail, we would like to elaborate the criteria adopted for labeling the interaction of methanol at various ZnO surfaces. For all the configurations reported in this study, we described molecular adsorption or dissociation of MeOH based on variation in its O-H bond-length, which is 0.97 Å in MeOH molecule. The physisorption is defined as slight elongation of O-H bond, from 0.97 Å to 0.98 Å. On the other hand, O-H bond elongation more than 0.99 Å is associated with chemisorption of MeOH on the facet. In all cases of O-H bond dissociation, the distance between O_{MeOH} and H is more than 1.45 Å (>50% of O-H bond-length). Also, the dissociated H atom binds to the surface oxygen atom with O-H distance varying between 0.98–1.06 Å, which infers bond formation between them. Although, interaction energy is used to define the thermodynamic stability of the resulting complex, it is not measure of observed bond activation. As will be discussed later, complexes with maximum activation or even dissociation are not always the ones with highest thermodynamic stability.

On the $(10\bar{1}0)$ facet, methanol adsorbs either molecularly or dissociatively at different sites. The interaction energy, O-H bond-length, and Zn-O_{MeOH} bond-length are tabulated in Table 1. Molecular adsorption of MeOH is thermodynamically the most probable outcome at this facet. However as seen from the Table 1, dissociation of MeOH into methoxy is also a likely product at elevated temperatures considering the small energy difference between these two outcomes. We report strong chemisorption and spontaneous dissociation of O-H bond of MeOH. A weak chemisorption is also observed, consistent with previously reported work [63], though it is not thermodynamically most favorable outcome. At this point, it is pertinent to note that a molecule like MeOH could be placed at the symmetry driven unique points on the surface in various different ways. A detail account of which could be found in our previous paper [33]. A small change in MeOH orientation wrt surface leads to completely different result in terms of extent of O-H bond elongation or even O-H bond dissociation. Considering this, any study of MeOH interaction is always limited by initial configurations one investigates and there is a dire need of formalizing a methodology for accounting of all possibilities.

Fig. 1 shows representative conformations of MeOH upon adsorption/dissociation on this facet. A closer look at the adsorbed conformations reveal certain patterns in MeOH interaction with the facet. For example, highly chemisorbed methanol always gets adsorbed through oxygen (refer Fig. 1-(b)) whereas in case of physisorbed MeOH, sometimes it gets adsorb through methylic H (refer Fig. 1-(c)). Adsorption through methylic H atom results in activation of C-H bond of MeOH. The C-H bond elongates to 4%. Consequently, the C-O bond strengthens (as shown in Table 1) and reduces to 1.39 Å which indicates partial oxidation of methanol. Another interesting observation is that MeOH adsorption also leads to the surface reconstruction which results into formation of voids as evident in all the cases. However, the extent of reconstruction depends on the outcome i.e. chemisorption (Fig. 1-(b) and (c)) or dissociation (Fig. 1-(d) and (e)). It was also observed that the dissociated methoxy group can adsorb at a Zn site or at bridge of two Zn sites. Further we investigate the interaction of MeOH with reconstructed surface by introducing second MeOH molecule with the most stable configuration. We placed the second molecule at various sites in the vicinity of previously chemisorbed MeOH. This results into two outcomes, viz. chemisorption and dissociation, depending on availability of oxygen atom near the second molecule for abstraction of proton of MeOH. Dissociation of O-H bond of second MeOH is thermodynamically the most favorable outcome of this interaction (as shown in Tab. SI1).

Another flat facet that we studied is $(11\bar{2}0)$. This is a highly symmetric facet with less number of inequivalent sites on the surface as shown in Fig. SI4-(a). Interestingly, when MeOH is placed on any sites except 4th, upon optimization it gets chemisorbed at one specific site as schematically represented in Fig. SI4-(b). The orientation of methanol on this site is shown in Fig. SI4-(c). E_{int} for methanol at this site is −1.24 eV and O-H bond of MeOH elongates to 1.02 Å. Further adsorbing the second MeOH molecule on the surface, results in chemisorption of molecule with elongation in O-H bond up to 1.03 Å. This shows that $(11\bar{2}0)$ facet does not favor dissociation of methanol due to uniformity on the surface. Comparing adsorption of MeOH on flat facets underlines the fact that nonuniform facet provides multiple possibilities.

Next we investigate a stepped facet $(10\bar{1}3)$. Various available unique sites, where MeOH is placed are shown in Fig. SI5-(a). Those sites where methanol/methoxy adsorb upon optimization are shown in Fig. SI5-(b). Interaction energy, O-H bond-length and Zn-O_{MeOH} bond-length are tabulated in Table 2. As evident from the interaction energy, dissociation of methanol is thermodynamically the most favorable outcome on this facet. Fig. 2 shows the representative cases of chemisorption as well as dissociation of methanol on $(10\bar{1}3)$ facet. It is observed that generally MeOH/methoxy group adsorb via its O at Zn site, but in few cases, it adsorbs through its methylic H (refer Fig. 2-(b)). Contrary to $(10\bar{1}0)$ facet, this methylic adsorption shows higher activation of O-H bond. Adsorption through methylic H leads to elongation of C-H bond by 7% accompanied with reduction in C-O bond to 1.37 Å as shown in Table 2. Elongation in C-H bond-length along with reduction in C-O bond-length is an evidence of partial oxidation of methanol at this stepped facet. The dissociated methoxy group adsorbs on the surface in two different ways, either through O_{MeOH} (monodentate as shown in Fig. 2-(c)) or via two atoms i.e. O_{MeOH} and methylic H (bidentate as shown in Fig. 2-(d)). Interestingly, coordination number of surface sites where MeOH/methoxy group adsorbs governs the stability of any configuration. Due to the presence of step, extent of reconstruction upon methanol adsorption is less on this facet as compared to $(10\bar{1}0)$ facet.

Next, we discuss another stepped facet $(11\bar{2}2)$ which is more symmetric than $(10\bar{1}3)$ facet. Methanol is placed at all available unique sites as shown schematically in Fig. SI6-(a) and its interaction with the ZnO surface has been studied. In majority of the cases, irrespective of initial positions of methanol, it diffuses to a single position upon optimization, as indicated by red triangle in Fig. SI6-(b). Similar to the previous stepped facet, this facet also shows two outcomes of MeOH interaction viz. dissociation as well as chemisorption. However, dissociation is highly favored over its molecular adsorption as evident from Table 3. Distinct conformations of adsorption as well as dissociation of methanol on this facet are shown in Fig. 3. A careful look at the adsorbed conformations reveals that depending on the sites of adsorption viz. bridge (refer Fig. 3-(a)) or on-top site (refer Fig. 3-(b)), elongation of O-H bond

Table 1
Interaction energy (eV), O-H bond-length (Å), C-O bond-length (Å), and Zn-O_{MeOH} bond-length (Å) for various sites on ZnO $(10\bar{1}0)$ facet. All these positions are indicated in Fig. SI3-(b). Dissociation is indicated in red color while molecular adsorption is shown in black color.

Positions	E_{int} (eV)	O-H BL (Å)	C-O BL (Å)	Zn-O_{MeOH} BL (Å)
4	−1.58	1.04	1.44	2.05
3	−1.52	1.03	1.44	2.06
7	−1.36	3.09	1.43	1.96
6	−1.35	4.37	1.41	1.96
5	−1.25	1.61	1.41	1.93
1	−1.08	0.98	1.45	2.11
2	−0.69	1.00	1.39	3.54

Table 2
Interaction energy (eV), O-H bond-length (Å), C-O bond-length (Å), and Zn-O_{MeOH} bond-length (Å) for various sites on ZnO $(10\bar{1}3)$ facet. All these position are indicated in Fig. SI5-(b). Dissociation of MeOH is shown in red color while molecular adsorption is shown in black color.

Positions	E_{int} (eV)	O-H BL (Å)	C-O BL (Å)	Zn-O_{MeOH} BL (Å)
2,7	−3.88	1.57	1.44	1.88
10	−3.70	1.73	1.39	1.89
6,8	−2.87	1.46	1.43	1.90
4,5,9	−1.71	1.03	1.37	3.49
1	−1.54	0.99	1.45	2.17
3	−1.42	0.99	1.45	2.21

Table 3
Interaction energy (eV), O-H bond-length (Å), C-O bond-length (Å), and Zn-O_{MeOH} bond-length (Å) for various sites on ZnO $(11\bar{2}2)$ facet. All these position are indicated in Fig. SI6-(b). Dissociation is indicated in red color while molecular adsorption is shown in black color.

Positions	E_{int} (eV)	O-H BL (Å)	C-O BL (Å)	Zn-O_{MeOH} BL (Å)
3,9	−6.24	2.25	1.44	1.98
1,2,7,11,12	−3.10	2.04	1.44	1.98
6,8	−2.95	2.01	1.45	1.99
13	−2.86	1.94	1.45	1.98
5	−1.78	1.00	1.45	2.04
10	−1.77	0.98	1.47	2.26
4	−1.56	0.98	1.46	2.08

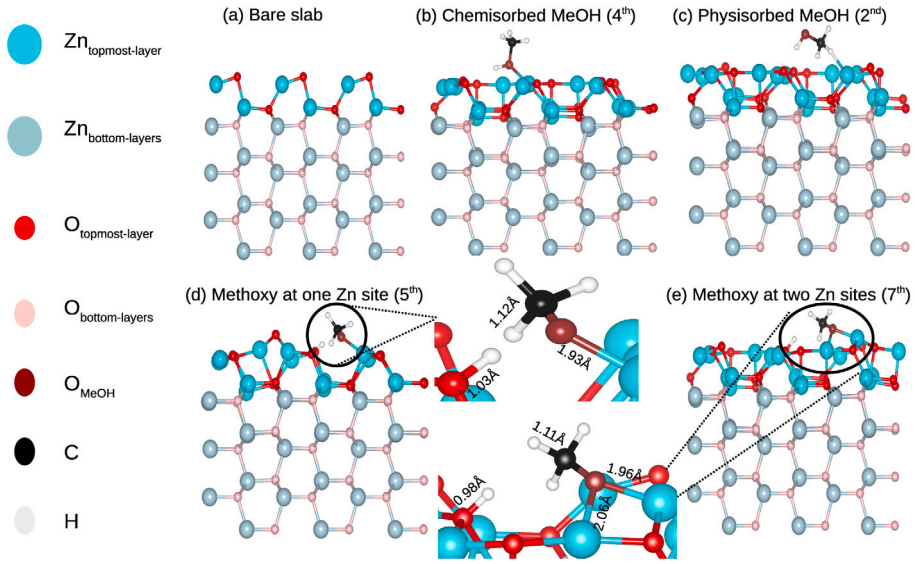

Fig. 1. (a) side view of bare $(10\bar{1}0)$ facet, (b) Chemisorbed MeOH with ~7% elongation of O-H bond, (c) chemisorbed MeOH with ~3% elongation of O-H bond, (d) dissociated MeOH with methoxy group attached to Zn atom, and (e) dissociated MeOH with methoxy group at bridge of two Zn atoms. For clear view of adsorption of methoxy on the surface (d) and (e) figures are enlarged. The numbers in the bracket indicates configuration with other details listed in Table 1.

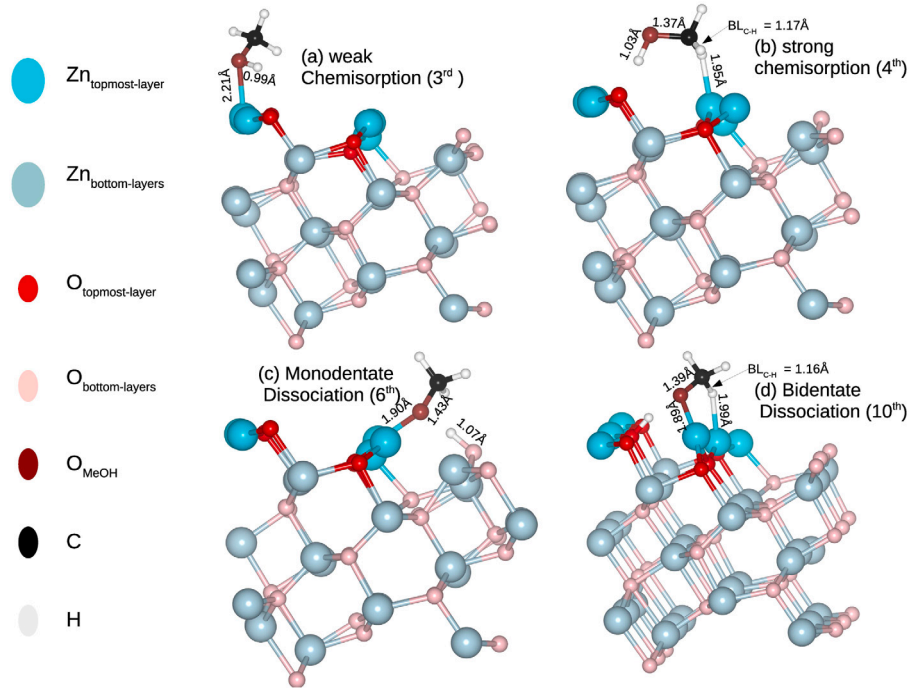

Fig. 2. Various conformers of MeOH interaction with $(10\bar{1}3)$ facet. Upper panel shows chemisorption of MeOH and lower panel shows dissociation of MeOH at the facet. (a) weak chemisorption, (b) strong chemisorption, (c) monodentate adsorption of methoxy group, and (d) bidentate adsorption of methoxy group. The numbers in the bracket indicates configuration and the details are listed in Table 2.

of methanol differs. The dissociated cases have methoxy adsorbed at Zn site with Zn-O_{MeOH} bond-length (1.98 Å) comparable to bulk Zn-O bond-length. Further, second molecule also chemisorbs on the surface with O-H bond elongation up to 1.01 Å. In short, dissociation of MeOH is thermodynamically the most favorable outcome on stepped facets while molecular adsorption is favorable on the flat facets.

So far, we have observed that different facets of ZnO interact differently with methanol resulting into molecular adsorption and/or activation and/or dissociation of O-H bond. This difference in behavior is correlated with underlying electronic structure of these facets. Coordination number and Mulliken charges of surface Zn and O atoms of all the facets are noted in Tab. SI2. For all facets but $(10\bar{1}3)$, all the surface Zn or O atoms are identical. $(10\bar{1}3)$ facet has two types of Zn and O atoms on the surface experiencing the difference in their neighboring environment and hence Mulliken charges. It is also evident that higher coordination of surface atoms leads to higher effective charges and hence reduced reactivity. For example, in the case of $(11\bar{2}0)$ facet, Zn and O atoms with highest coordination and Mulliken charges do not show dissociation of methanol. The inhibition of O-H bond breaking of MeOH at $(11\bar{2}0)$ facet could be explained by analyzing the total density of states (*tDOS*) plot as shown in Fig. 4. The *tDOS* plot for $(11\bar{2}0)$ facet clearly shows non availability of energy states near Fermi level, which makes it least reactive. Remaining all facets with energy states available near Fermi level enhance reactivity of the facet and explain

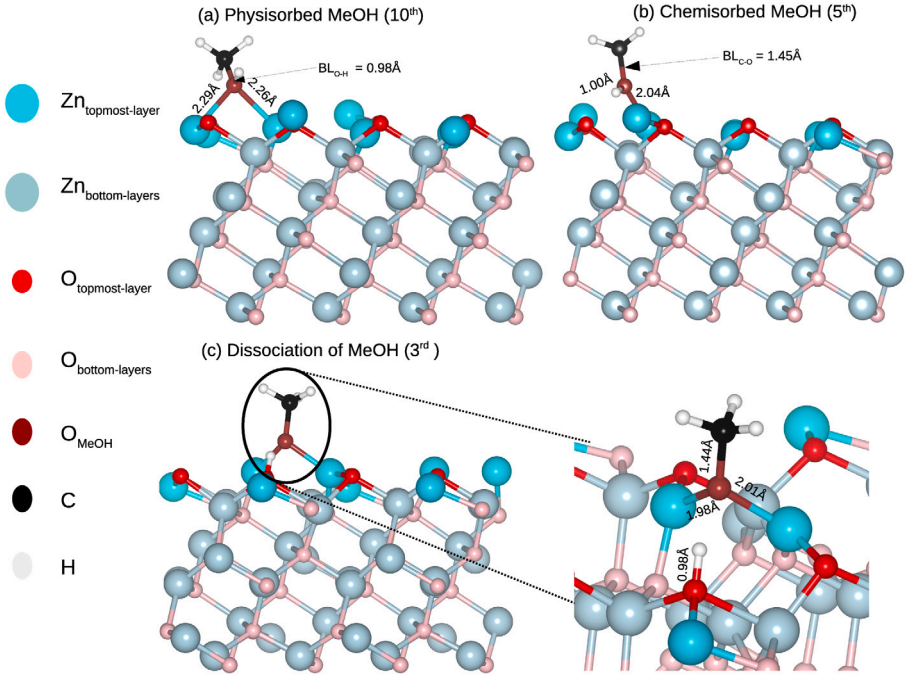

Fig. 3. Upper panel shows adsorption of MeOH at (11$\bar{2}$2) facet and lower panel shows dissociation of MeOH. (a) physisorbed MeOH (b) chemisorbed MeOH (c) adsorption of methoxy group at bridge of two Zn atoms. The enlarged figure is shown to provide a clear view of methoxy group adsorption on Zn site. The numbers in the bracket indicates configuration and the details are listed in Table 3.

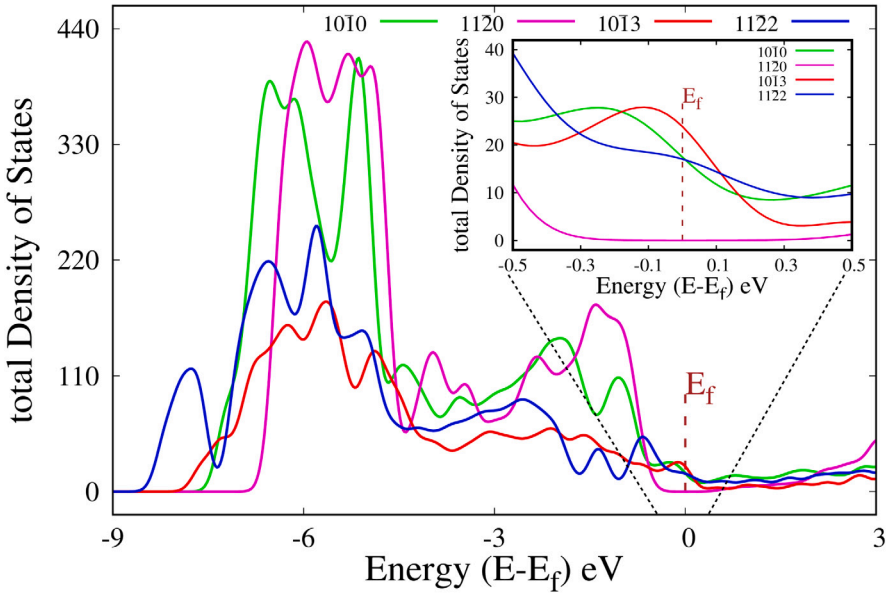

Fig. 4. The *tDOS* of four facets are plotted. The inset figure shows the enlarged *tDOS* near Fermi level. Only for (11$\bar{2}$0) facet *tDOS* is zero at Fermi.

the observed dissociation of methanol on these facets. Next we plot projected density of states (*pDOS*) of surface atoms for all facets. 3*d* and 4*s* states of surface Zn atoms are shown in Fig. 5. Zn, being a late transition metal with fully filled 3*d* states lying much below the Fermi level (refer Fig. 5-a), does not participate in reactivity. While its 4*s* states, lying near the Fermi level, participate in reactivity of the surface. It is clearly seen in Fig. 5-b that for flat facets, 4*s* states of surface Zn atoms are zero near Fermi level while it is non-zero for stepped facets. The presence of non-zero 4*s* states near Fermi for stepped facets favors dissociation of MeOH, which is most favorable on these facets.

4. Conclusion

ZnO is considered as a very active catalyst for many reactions because of its mixed covalent and ionic bonding. As evident from XRD, there are various prominent facets in ZnO and only few facets have been studied for methanol adsorption. We have carried out a systematic study of methanol adsorption on various facets of ZnO which includes two flat [(10$\bar{1}$0) and (11$\bar{2}$0)] and two stepped [(10$\bar{1}$3) and (11$\bar{2}$2)] surfaces. O-H bond dissociation is thermodynamically the most favorable outcome on stepped facets where on chemisorption of MeOH with 7%–10% O-H bond activation is observed on the flat facets. We also report considerable surface reconstruction upon MeOH adsorption. However,

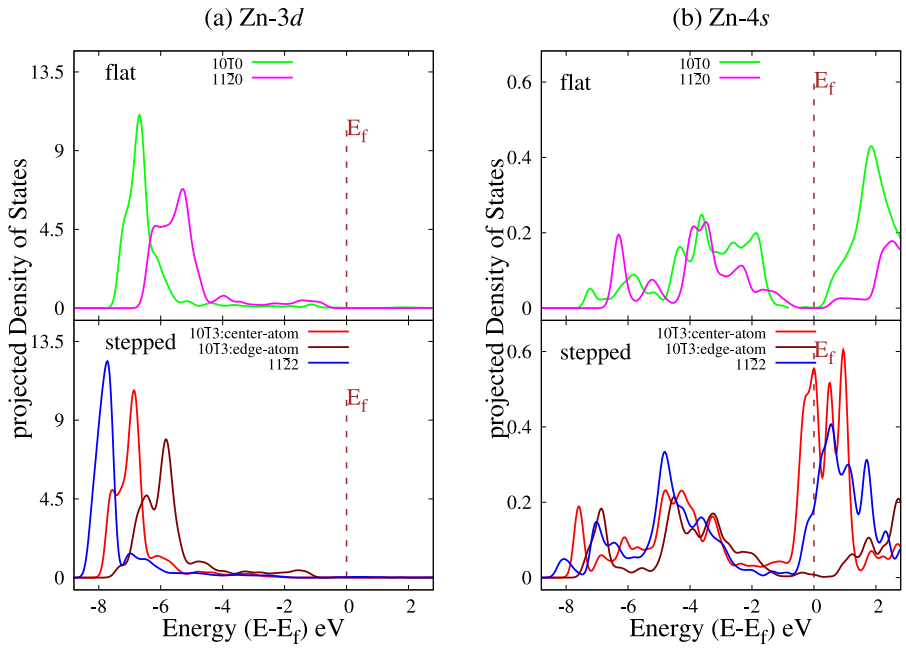

Fig. 5. (a) *pDOS* of Zn-3*d* orbitals of flat and stepped facets. As expected, 3*d* in Zn being completely filled are much away from Fermi level. (b) Zn-4*s* of flat and stepped facets. It is interesting to note that for flat facets *pDOS* of surface Zn atoms show unavailability of states near Fermi as opposed to case of stepped facet.

the reconstruction is lesser on the stepped surfaces compared to the flat facets. Further, partial oxidation of MeOH is favored on ZnO facets. Our detailed electronic structure analysis brings out the rationale behind the surface dependent interaction of MeOH. Analysis of pDOS, tDOS along with Mulliken charges on surface atoms explains the facet dependent reactivity observed in case of ZnO. Facets with available empty states near Fermi leads to O-H bond dissociation whereas absence of empty states near Fermi leads to O-H bond activation. Considering the role of ZnO in various reactions and importance of MeOH in the current energy scenario we believe our study shade light on some important aspects of interaction of ZnO with MeOH. Finally, ZnO is a known catalyst for synthesis of MeOH. Our work opens up a possibility of ZnO as a catalyst for MeOH dissociation as well which awaits experimental verification.

CRediT authorship contribution statement

Shweta Mehta: Methodology, Validation, Analysis, Writing – original draft. **Kavita Joshi:** Conceptualization, Writing – review & editing, Project administration, Supervision.

Declaration of competing interest

The authors declare that they have no known competing financial interests or personal relationships that could have appeared to influence the work reported in this paper.

Acknowledgments

CSIR-4PI is gratefully acknowledged for the computational facility. SM acknowledges UGC for research fellowship.

Appendix A. Supplementary data

Supplementary material related to this article can be found online at https://doi.org/10.1016/j.apsusc.2022.154150.

References

[1] G.A. Olah, Beyond oil and gas: The methanol economy, Angew. Chem. Int. Ed. 44 (18) (2005) 2636–2639, http://dx.doi.org/10.1002/anie.200462121, arXiv:https://onlinelibrary.wiley.com/doi/pdf/10.1002/anie.200462121. URL https://onlinelibrary.wiley.com/doi/abs/10.1002/anie.200462121.

[2] J. Kothandaraman, A. Goeppert, M. Czaun, G.A. Olah, G.S. Prakash, Conversion of CO_2 from air into methanol using a polyamine and a homogeneous ruthenium catalyst, J. Am. Chem. Soc. 138 (3) (2016) 778–781.

[3] L.-N. Chen, K.-P. Hou, Y.-S. Liu, Z.-Y. Qi, Q. Zheng, Y.-H. Lu, J.-Y. Chen, J.-L. Chen, C.-W. Pao, S.-B. Wang, Y.-B. Li, S.-H. Xie, F.-D. Liu, D. Prendergast, L.E. Klebanoff, V. Stavila, M.D. Allendorf, J. Guo, L.-S. Zheng, J. Su, G.A. Somorjai, Efficient hydrogen production from methanol using a single-site Pt1/CeO_2 catalyst, J. Am. Chem. Soc. 141 (45) (2019) 17995–17999, http://dx.doi.org/10.1021/jacs.9b09431, PMID: 31647653. arXiv:https://doi.org/10.1021/jacs.9b09431.

[4] S.J. Blanksby, G.B. Ellison, Bond dissociation energies of organic molecules, Acc. Chem. Res. 36 (4) (2003) 255–263.

[5] C. Ammon, A. Bayer, G. Held, B. Richter, T. Schmidt, H.-P. Steinrück, Dissociation and oxidation of methanol on Cu (110), Surf. Sci. 507 (2002) 845–850.

[6] Q. Sun, B. Shen, K. Fan, J. Deng, Roles of surface and subsurface oxygen in the dehydrogenation of methanol on silver surface, Chem. Phys. Lett. 322 (1–2) (2000) 1–8.

[7] B. Xu, J. Haubrich, T.A. Baker, E. Kaxiras, C.M. Friend, Theoretical study of O-assisted selective coupling of methanol on Au (111), J. Phys. Chem. C 115 (9) (2011) 3703–3708.

[8] Y. Ishikawa, M.-S. Liao, C.R. Cabrera, Oxidation of methanol on platinum, ruthenium and mixed Pt–M metals (M=Ru, Sn): a theoretical study, Surf. Sci. 463 (1) (2000) 66–80.

[9] C. Zhang, P. Hu, A first principles study of methanol decomposition on Pd (111): mechanisms for O–H bond scission and C–O bond scission, J. Chem. Phys. 115 (15) (2001) 7182–7186.

[10] G.-C. Wang, Y.-H. Zhou, Y. Morikawa, J. Nakamura, Z.-S. Cai, X.-Z. Zhao, Kinetic mechanism of methanol decomposition on Ni (111) surface: a theoretical study, J. Phys. Chem. B 109 (25) (2005) 12431–12442.

[11] S. Yanagisawa, T. Tsuneda, K. Hirao, Y. Matsuzaki, Theoretical investigation of adsorption of organic molecules onto Fe (110) surface, J. Mol. Struct.: Theochem. 716 (1–3) (2005) 45–60.

[12] R. Jiang, W. Guo, M. Li, H. Zhu, L. Zhao, X. Lu, H. Shan, Methanol dehydrogenation on Rh (1 1 1): A density functional and microkinetic modeling study, J. Mol. Catal. A 344 (1–2) (2011) 99–110.

[13] X. Bao, M. Muhler, B. Pettinger, R. Schlögl, G. Ertl, On the nature of the active state of silver during catalytic oxidation of methanol, Catal. Lett. 22 (3) (1993) 215–225.

[14] J. Greeley, M. Mavrikakis, Methanol decomposition on Cu (111): a DFT study, J. Catal. 208 (2) (2002) 291–300.

[15] O.R. de la Fuente, M. Borasio, P. Galletto, G. Rupprechter, H.-J. Freund, The influence of surface defects on methanol decomposition on Pd (111) studied by XPS and PM-IRAS, Surf. Sci. 566 (2004) 740–745.

[16] O. Skoplyak, C.A. Menning, M.A. Barteau, J.G. Chen, Experimental and theoretical study of reactivity trends for methanol on Co/ Pt (111) and Ni/ Pt (111) bimetallic surfaces, J. Chem. Phys. 127 (11) (2007) 114707.

[17] V. Orazi, P. Bechthold, P.V. Jasen, R. Faccio, M.E. Pronsato, E.A. Gonzalez, DFT study of methanol adsorption on PtCo (111), Appl. Surf. Sci. 420 (2017) 383–389.

[18] L.T. Sein Jr., S.A. Jansen, DFT study of the adsorption and dissociation of methanol on NiAl (100), J. Catal. 196 (2) (2000) 207–211.

[19] Ø. Borck, I.-H. Svenum, A. Borg, Adsorption of methanol and methoxy on NiAl (110) and Ni_3Al (111): A DFT study, Surf. Sci. 603 (16) (2009) 2378–2386.

[20] P. Du, P. Wu, C. Cai, Mechanism of methanol decomposition on the Pt_3Ni (111) surface: DFT study, J. Phys. Chem. C 121 (17) (2017) 9348–9360.

[21] S.B. Dalavi, S. Agarwal, P. Deshpande, K. Joshi, B.L.V. Prasad, Disordered but efficient: Understanding the role of structure and composition of the Co–Pt alloy on the electrocatalytic methanol oxidation reaction, J. Phys. Chem. C 125 (14) (2021) 7611–7624, http://dx.doi.org/10.1021/acs.jpcc.0c10165, arXiv:https://doi.org/10.1021/acs.jpcc.0c10165.

[22] F. Mehmood, J. Greeley, P. Zapol, L.A. Curtiss, Comparative density functional study of methanol decomposition on Cu_4 and Co_4 clusters, J. Phys. Chem. B 114 (45) (2010) 14458–14466.

[23] R.J. Gasper, A. Ramasubramaniam, Density functional theory studies of the methanol decomposition reaction on graphene-supported Pt_{13} nanoclusters, J. Phys. Chem. C 120 (31) (2016) 17408–17417.

[24] Z.-J. Zuo, L. Wang, P.-D. Han, W. Huang, Insight into the size effect on methanol decomposition over Cu-based catalysts based on density functional theory, Comput. Theor. Chem. 1033 (2014) 14–22.

[25] K. Ghatak, T. Sengupta, S. Krishnamurty, S. Pal, Computational investigation on the catalytic activity of Rh_6 and Rh_4 Ru_2 clusters towards methanol activation, Theor. Chem. Account. 134 (1) (2015) 1–11.

[26] H. Petitjean, K. Tarasov, F. Delbecq, P. Sautet, J.M. Krafft, P. Bazin, M.C. Paganini, E. Giamello, M. Che, H. Lauron-Pernot, et al., Quantitative investigation of MgO Brønsted basicity: DFT, IR, and calorimetry study of methanol adsorption, J. Phys. Chem. C 114 (7) (2010) 3008–3016.

[27] Z. Liu, C.C. Sorrell, P. Koshy, J.N. Hart, DFT study of methanol adsorption on defect-free CeO_2 low-index surfaces, ChemPhysChem 20 (16) (2019) 2074–2081.

[28] Ø. Borck, E. Schröder, First-principles study of the adsorption of methanol at the α-Al_2O_3 (0001) surface, J. Phys.: Condens. Matter 18 (1) (2005) 1.

[29] Ø. Borck, E. Schröder, Adsorption of methanol and methoxy on the α-Cr_2O_3 (0001) surface, J. Phys.: Condens. Matter 18 (48) (2006) 10751.

[30] W. Liu, J.-g. Wang, X. Guo, W. Fang, M. Wei, X. Lu, L. Lu, Dissociation of methanol on hydroxylated TiO_2-B (100) surface: Insights from first principle DFT calculation, Catal. Today 165 (1) (2011) 32–40.

[31] T. Choksi, J. Greeley, Partial oxidation of methanol on MoO_3 (010): A DFT and microkinetic study, ACS Catal. 6 (11) (2016) 7260–7277.

[32] A. Kumar, R. Kumar, R. Singh, B. Prasad, D. Kumar, M. Kumar, Biosynthesis of ZnO nanoparticles and effect of silver doping in gas sensing characteristics of volatile organic compounds, J. Coat. Technol. Res. (2021) 1–13.

[33] S. Mehta, S. Agarwal, N. Kenge, S.P. Mekala, V. Patil, T. Raja, K. Joshi, Mixed metal oxide: A new class of catalyst for methanol activation, Appl. Surf. Sci. 534 (2020) 147449.

[34] J. Andzelm, N. Govind, G. Fitzgerald, A. Maiti, DFT study of methanol conversion to hydrocarbons in a zeolite catalyst, Int. J. Quantum Chem. 91 (3) (2003) 467–473.

[35] C. Wang, Y. Chu, A. Zheng, J. Xu, Q. Wang, P. Gao, G. Qi, Y. Gong, F. Deng, New insight into the hydrocarbon-pool chemistry of the methanol-to-olefins conversion over zeolite H-ZSM-5 from GC-MS, solid-state NMR spectroscopy, and DFT calculations, Chem. Eur. J. 20 (39) (2014) 12432–12443.

[36] M.F. Fellah, I. Onal, DFT study of direct methanol oxidation to formaldehyde by N_2O on the $[Fe]^{2+}$–ZSM-5 zeolite cluster, J. Phys. Chem. C 116 (25) (2012) 13616–13622.

[37] A.O. Elnabawy, R. Schimmenti, A. Cao, J.K. Nørskov, Why ZnO is the support for cu in methanol synthesis? A systematic study of the strong metal support interactions, ACS Sustain. Chem. Eng. 10 (4) (2022) 1722–1730, http://dx.doi.org/10.1021/acssuschemeng.1c07980, arXiv:https://doi.org/10.1021/acssuschemeng.1c07980.

[38] B. Meyer, D. Marx, Density-functional study of the structure and stability of ZnO surfaces, Phys. Rev. B 67 (3) (2003) 035403.

[39] A. Boisen, S. Dahl, J.K. Nørskov, C.H. Christensen, Why the optimal ammonia synthesis catalyst is not the optimal ammonia decomposition catalyst, J. Catal. 230 (2) (2005) 309–312, http://dx.doi.org/10.1016/j.jcat.2004.12.013, URL https://www.sciencedirect.com/science/article/pii/S0021951704006013.

[40] C.T. Vo, L.K. Huynh, J.-Y. Hung, J.-C. Jiang, Methanol adsorption and decomposition on ZnO $(10\bar{1}0)$ surface: A density functional theory study, Appl. Surf. Sci. 280 (2013) 219–224.

[41] N. Abedi, P. Herrmann, G. Heimel, Methanol on ZnO $(10\bar{1}0)$: From adsorption over initial dehydrogenation to monolayer formation, J. Phys. Chem. C 119 (37) (2015) 21574–21584, http://dx.doi.org/10.1021/acs.jpcc.5b07154, arXiv:https://doi.org/10.1021/acs.jpcc.5b07154.

[42] S. Ruan, Z. Li, H. Shi, W. Wang, X. Ren, X. Shao, Identifying different adsorption states of methanol on ZnO$(10\bar{1}0)$: A scanning tunneling microscopy and density functional theory study, J. Phys. Chem. C 123 (14) (2019) 9105–9111, http://dx.doi.org/10.1021/acs.jpcc.9b00576, arXiv:https://doi.org/10.1021/acs.jpcc.9b00576.

[43] G.K. Smith, S. Lin, W. Lai, A. Datye, D. Xie, H. Guo, Initial steps in methanol steam reforming on PdZn and ZnO surfaces: Density functional theory studies, Surf. Sci. 605 (7–8) (2011) 750–759.

[44] L. Jin, Y. Wang, Surface chemistry of methanol on different ZnO surfaces studied by vibrational spectroscopy, Phys. Chem. Chem. Phys. 19 (20) (2017) 12992–13001.

[45] P.E. Blöchl, Projector augmented-wave method, Phys. Rev. B 50 (24) (1994) 17953–17979.

[46] G. Kresse, D. Joubert, From ultrasoft pseudopotentials to the projector augmented-wave method, Phys. Rev. B 59 (3) (1999) 1758–1775.

[47] J.P. Perdew, K. Burke, M. Ernzerhof, Generalized gradient approximation made simple, Phys. Rev. Lett. 77 (18) (1996) 3865–3868.

[48] J.P. Perdew, K. Burke, M. Ernzerhof, Generalized gradient approximation made simple, Phys. Rev. Lett. 78 (7) (1997) 1396; Phys. Rev. Lett. 77 (1996) 3865.

[49] G. Kresse, J. Hafner, *Ab initio* molecular-dynamics simulation of the liquid-metal–amorphous-semiconductor transition in germanium, Phys. Rev. B 49 (20) (1994) 14251–14269.

[50] G. Kresse, J. Furthmüller, Efficient iterative schemes for *ab initio* total-energy calculations using a plane-wave basis set, Phys. Rev. B 54 (16) (1996) 11169–11186.

[51] G. Kresse, J. Furthmüller, Efficiency of ab-initio total energy calculations for metals and semiconductors using a plane-wave basis set, Comput. Mater. Sci. 6 (1) (1996) 15–50.

[52] A. Jain, S.P. Ong, G. Hautier, W. Chen, W.D. Richards, S. Dacek, S. Cholia, D. Gunter, D. Skinner, G. Ceder, et al., Commentary: The materials project: A materials genome approach to accelerating materials innovation, Appl. Mater. 1 (1) (2013) 011002.

[53] R.R. Reeber, Lattice parameters of ZnO from 4.2 to 296 K, J. Appl. Phys. 41 (13) (1970) 5063–5066.

[54] E.M. Flores, M.L. Moreira, M.J. Piotrowski, Structural and electronic properties of bulk ZnX (X=O, S, Se, Te), ZnF_2, and ZnO/ZnF_2: A DFT investigation within PBE, PBE+ U, and hybrid HSE functionals, J. Phys. Chem. A 124 (19) (2020) 3778–3785.

[55] D. Stradi, L. Jelver, S. Smidstrup, K. Stokbro, Method for determining optimal supercell representation of interfaces, J. Phys.: Condens. Matter 29 (18) (2017) 185901.

[56] S. Grimme, Semiempirical GGA-type density functional constructed with a long-range dispersion correction, J. Comput. Chem. 27 (15) (2006) 1787–1799.

[57] R. Dronskowski, P.E. Blöchl, Crystal orbital Hamilton populations (COHP): energy-resolved visualization of chemical bonding in solids based on density-functional calculations, J. Phys. Chem. 97 (33) (1993) 8617–8624.

[58] V.L. Deringer, A.L. Tchougréeff, R. Dronskowski, Crystal orbital Hamilton population (COHP) analysis as projected from plane-wave basis sets, J. Phys. Chem. A 115 (21) (2011) 5461–5466.

[59] S. Maintz, V.L. Deringer, A.L. Tchougréeff, R. Dronskowski, Analytic projection from plane-wave and PAW wavefunctions and application to chemical-bonding analysis in solids, J. Comput. Chem. 34 (29) (2013) 2557–2567.

[60] S. Maintz, V.L. Deringer, A.L. Tchougréeff, R. Dronskowski, LOBSTER: A tool to extract chemical bonding from plane-wave based DFT, J. Comput. Chem. 37 (11) (2016) 1030–1035.

[61] O. Dulub, L.A. Boatner, U. Diebold, STM study of the geometric and electronic structure of ZnO (0001)-Zn,(0001)-o,$(10\bar{1}0)$, and $(11\bar{2}0)$ surfaces, Surf. Sci. 519 (3) (2002) 201–217.

[62] U. Diebold, L.V. Koplitz, O. Dulub, Atomic-scale properties of low-index ZnO surfaces, Appl. Surf. Sci. 237 (1) (2004) 336–342, http://dx.doi.org/10.1016/j.apsusc.2004.06.040, Proceedings of the Seventh International Symposium on Atomically Controlled Surfaces, Interfaces and Nanostructures. URL https://www.sciencedirect.com/science/article/pii/S0169433204009857.

[63] R.G.S. Pala, H. Metiu, Selective promotion of different modes of methanol adsorption via the cation substitutional doping of a ZnO$(10\bar{1}0)$ surface, J. Catal. 254 (2) (2008) 325–331, http://dx.doi.org/10.1016/j.jcat.2008.01.014, URL https://www.sciencedirect.com/science/article/pii/S0021951708000158.